Water Resources Research

RESEARCH ARTICLE
10.1029/2024WR039392

Water Transit Time Explains the Concentration, Quality and Reactivity of Dissolved Organic Carbon in an Alpine Stream

G. Grandi[1], N. Catalán[2], S. Bernal[3], C. Fasching[4], T. I. Battin[5], and E. Bertuzzo[1]

[1]Department of Environmental Sciences, Informatics and Statistics, University of Venice Ca' Foscari, Venice, Italy, [2]Institute of Environmental Assessment and Water Research (IDAEA-CSIC), University of Barcelona, Barcelona, Spain, [3]Centre of Advanced Studies of Blanes (CEAB-CSIC), University of Blanes, Blanes, Spain, [4]Department of Geography, Philipps-University Marburg, Marburg, Germany, [5]Ecole Polytechnique Fédérale de Lausanne, Lausanne, Switzerland

Abstract The amount and quality of dissolved organic carbon (DOC) exported from terrestrial to riverine ecosystems are critical factors influencing aquatic metabolism and ecosystem health in streams, rivers, and lakes. This study investigates the interplay between hydrologic conditions and DOC dynamics in an alpine catchment, focusing on how DOC concentration and quality shift during baseflow, snowmelt, and storm events. Such dynamics were explored in the Oberer Seebach basin (Austria) where sub-daily DOC concentration data, along with high resolution excitation-emission matrices and absorbance spectra, were used to characterize DOC concentration and quality. We quantitatively linked hydrologic pathways with DOC dynamics by advancing a framework that couples water age, which tracks the time water spends within the catchment, with the Reactivity Continuum model, which quantifies the evolution of DOC reactivity and ensuing concentration. Results show that simulating both water age and DOC reactivity effectively reproduces DOC concentrations and reveals a correlation between modeled reactivity and observed DOC quality indices. During snowmelt and storm events, rapid hydrologic pathways transport reactive DOC with a quality profile similar to that of freshly formed terrestrial DOC, while during baseflow, slower pathways carry less reactive DOC with a signature of preceding degradation processes. These findings shed light on the role of catchment hydrology in carbon cycling and on its implications for riverine ecosystem functioning.

Plain Language Summary The critical zone, where soil, water, and the atmosphere meet, plays a vital role in moving and transforming organic matter as it flows through the landscape. In this study, we examined how different hydrologic conditions—such as baseflow, snowmelt, and storms—affect the quantity and quality of dissolved organic carbon (DOC) exported from soil into an alpine stream in Austria. We found that during snowmelt and storm events, water flows quickly through the soil, carrying reactive, fresh DOC. In contrast, under baseflow conditions, water spends more time in the soil, and the DOC it transports is less reactive, with signs of prior microbial degradation.

Key Points:

- PARAFAC analysis reveals distinct DOC signatures for different hydrologic regimes
- Water age and reactivity continuum approaches are combined to predict DOC concentration and reactivity in an alpine catchment
- The age of the water controls quality and reactivity of riverine DOC

Supporting Information:

Supporting Information may be found in the online version of this article.

Correspondence to:

E. Bertuzzo,
enrico.bertuzzo@unive.it

Citation:

Grandi, G., Catalán, N., Bernal, S., Fasching, C., Battin, T. I., & Bertuzzo, E. (2025). Water transit time explains the concentration, quality and reactivity of dissolved organic carbon in an alpine stream. *Water Resources Research*, *61*, e2024WR039392. https://doi.org/10.1029/2024WR039392

Received 6 NOV 2024
Accepted 3 MAR 2025

Author Contributions:

Conceptualization: G. Grandi, N. Catalán, S. Bernal, T. I. Battin, E. Bertuzzo
Data curation: G. Grandi, N. Catalán, C. Fasching, T. I. Battin
Formal analysis: G. Grandi
Investigation: G. Grandi
Methodology: G. Grandi, N. Catalán, S. Bernal, C. Fasching, E. Bertuzzo
Supervision: E. Bertuzzo
Visualization: G. Grandi
Writing – original draft: G. Grandi, E. Bertuzzo
Writing – review & editing: G. Grandi, N. Catalán, S. Bernal, C. Fasching, T. I. Battin, E. Bertuzzo

1. Introduction

Inland waters and the coastal oceans receive large quantities of organic carbon from terrestrial ecosystems (Battin et al., 2023), with dissolved organic carbon (DOC) being one of its main forms. DOC is a main driver of riverine ecosystem functioning and biogeochemical balance because its concentration and quality influences aquatic metabolism (Battin et al., 2023; Houser et al., 2003) and the transport of metals and pollutants (Bolan et al., 2011; Gros et al., 2021; Shanley et al., 2008). Through superficial and sub-superficial hydrologic pathways, DOC is drained from soils to streams and rivers, and either transported downstream to coastal oceans or respired by stream biota and emitted to the atmosphere as C dioxide (CO_2) and methane (Battin et al., 2009, 2023; Cole et al., 2007). Thus, freshwaters play a key role in regulating the global C cycle, connecting C pools in soil, water and atmosphere, and actively contributing to the production, transport, and transformation of DOC. A key step to understand and describe these biogeochemical processes is to characterize the temporal variability of lateral fluxes of DOC delivered from soil to river and stream networks. In order to predict the fate of DOC in the aquatic environment, it is also crucial to assess the quality and reactivity of the DOC mixture exported from soil and its degree of processing (Gentine et al., 2019; Kaplan et al., 2006).

Mountainous catchments play a crucial role in the regional and global carbon cycle. Previous studies have shown that snow and glacial snowmelt provide highly bioavailable DOC to streams (Hemingway et al., 2019; Hood et al., 2015) thus facilitating CO_2 evasion in headwater catchments (Horgby et al., 2019). Disentangling carbon fluxes in mountainous catchments is particularly challenging given the high intrinsic spatial and temporal heterogeneity of hydrologic pathways connecting soils to streams. Frozen soils and snowpacks can disconnect the river network from terrestrial DOC sources in winter, while large quantities of fresh DOC and nutrients are flushed during spring snowmelt (Boyer et al., 1997; Carey, 2003; Shatilla & Carey, 2019; Ulseth et al., 2018). Moreover, high-altitude landscapes are highly sensitive to global warming, and are already experiencing severe alterations of their hydrologic (Barnett et al., 2005; Hanus et al., 2021) and biogeochemical (Battin et al., 2023; Robison et al., 2023; Wrona et al., 2016) cycles.

Hydrology imposes a strong control on riverine DOC dynamics: a great share of the flux of DOC from terrestrial to fluvial ecosystems is actually exported during few intense precipitation and flow events (Raymond & Saiers, 2010). Experimental evidence shows that discharge, rather than ecological and biogeochemical factors, is the primary control on fluvial DOC concentration and flux exported by river networks (Dawson et al., 2008; Fasching et al., 2016). In alpine catchments, DOC riverine concentration usually peaks during the spring snowmelt (Carey, 2003; Wen et al., 2020). In these relatively short periods the export of DOC from soil to the river network can account for up to 55%–69% of the annual flux (Carey, 2003; Finlay et al., 2006).

As freshwater DOC is a complex mixture of numerous molecules with different chemical proprieties and behavior, it is not only essential to describe the short and long term variations of its riverine concentration, but also to capture its composition and reactivity in order to disentangle C dynamics within the aquatic environment. Some of the DOC constituents are directly accessible to be mineralized by microbial heterotrophic organisms (Battin et al., 2009; Cole et al., 2007). Other constituents require previous steps whether biological (e.g., enzymatic activities) or physical-chemical (e.g., UV-light) prior to their degradation and eventual mineralization. Moreover, some compounds persist in the river flow without being further degraded and exhibit a transport behavior similar to that of a conservative solute. The preponderance of the constituents of such reactivity spectrum is determined by the DOC sources and by the story of previous degradation processes. Besides the dynamics of its own degradation, DOC quality affects also other stream functions. For instance, soil-derived DOC is typically aromatic and colored and can decrease light penetration and, in turn, water temperature, autotrophic growth, chlorophyll concentration and primary productivity (Kowalczuk et al., 2006; Maritorena et al., 2002; Snucins & Gunn, 2000).

DOC formed in organic-rich superficial soil layers is transported to streams and rivers through hydrologic pathways. Along the way, DOC can undergo transformation and degradation. Its export dynamics are therefore controlled by two main factors: its initial composition, which influences the type and rate of transformation processes, and the time water and DOC spend within soils, which dictates the duration available for these transformations. We hypothesize that fast hydrologic pathways transport fresh DOC with a quality profile similar to that of newly formed terrestrial DOC, while DOC transported via slower pathways bears the signatures of preceding degradation processes. To test these hypotheses, we utilized data collected from the Oberer Seebach basin (OSB), an alpine catchment in Austria, where sub-daily observations of hydrologic and biochemical variables were recorded by Fasching et al. (2016). Excitation/emission matrices (EEMs) and absorbance spectra were used to calculate DOC quality indexes, enabling us to profile DOC quality under different hydrologic conditions, such as baseflow, snowmelt, and summer storms.

We applied the mathematical framework proposed in Grandi and Bertuzzo (2022) to quantitatively investigate the relation among hydrologic variability, water age and DOC degradation in the OSB. This approach aims at simulating DOC export from soils to streams and rivers by considering two main processes: (a) the biogeochemical transformation of DOC occurring during the transport process and (b) the time spent by water within the catchment. The first is quantified defining the initial concentration and reactivity distribution of the DOC carried by water that flows through organic-rich superficial soil layers during precipitation events, and estimating its degradation along the pathway applying the Reactivity Continuum (RC) model; the second is dictated by the Transit Time Distribution (TTD) of the water parcels leaving the catchment as discharge. The general expectation is that labile DOC components are quickly degraded, and thus, the longer the water travels within the catchment, the more degraded and less reactive the pool of exported DOC becomes.

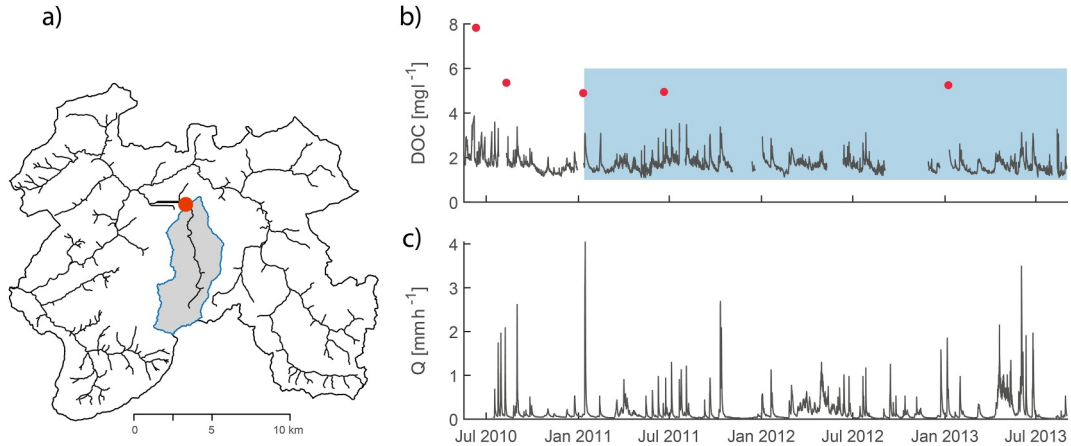

Figure 1. (a) Ybbs basin and the Oberer Seebach (OSB) subcatchment (gray area), Austria. Red circle indicates the location of the Lunz am See meteorological station and the sampling site for discharge and stream water samples. (b) stream DOC concentration time series, red dots indicate the samples removed from the raw dataset, while the blue box shows the time-window for which fluorescence and absorbance measurements were available. (c) discharge time series.

Tracking the distribution of reactivity of the DOC mixture along the flowpath enables the determination of its overall degradation rate. This feature was used in the previous application to predict the bulk DOC concentration observed in streamwater (Grandi & Bertuzzo, 2022). In this study instead, we fully exploit the framework's capabilities by comparing also the predicted DOC reactivity with quality indexes derived from EEMs and absorbance spectra, a feature made possible by the unprecedented richness of the OSB dataset. This approach allowed us to investigate the relationship between DOC quality, reactivity, and water transit time under the multifaceted hydrologic conditions of alpine environments.

The characteristics of the study area, dominated by an alpine climate, prompted us to develop and implement several model improvements compared to its previous formulation (Grandi & Bertuzzo, 2022). Specifically, we accounted for snowpack and snowmelt dynamics using a degree-day approach; implemented a time-variant form of the StorAge Selection (SAS) function, which is necessary to define the transit time distributions (TTDs) (Rinaldo et al., 2015); and formalized a scheme that allows for a more flexible suite of initial reactivity distributions while preserving the same analytical tractability.

2. Materials and Methods

2.1. Site and Data

Oberer Seebach is a pristine, second-order alpine stream located in Lower Austria, draining a karsic area of approx. 25 km^2 and with an outlet located at 600 m above sea level. Catchment surface is mostly covered by forests including the typical alpine vegetation: *Fraxinus excelsior*, *Acer pseudoplatanus*, *Fagus sylvatica*, *Salix caprea*, and *Picea abies*. Surface geology is dominated by the presence of glacial deposits, while deeper layers consist of calcareous rocks originated from lake sediments. OSB streambed is composed by gravel with a mean size of 23 mm, which determines an overall high porosity (approx. 29%). Discharge regimes are seasonally shaped by snow accumulation and snowmelt, resulting in frequent peak-flow events in spring and low-flow in winter. Long-term meteorological data and previous campaigns have found the annual precipitation to average 1,608 mm, while annual air and water temperature average respectively 7.4 and 6.7 °C. The hydrologic regime is dominated by snowmelt, which accounts for about 50% of the runoff, depending on the year (Ulseth et al., 2018). For a detailed description of the site geology, vegetation, hydrology, and climate the reader can refer to previous studies conducted in the region (Battin, 1999; Bretschko, 1991; Leichtfried, 1996).

Extensive hydrologic and biogeochemical monitoring was carried out by Fasching et al. (2016). The dataset of interest for this study comprises DOC riverine concentration observations collected every 6-hr from 17 May 2010 to 31 August 2013 (4,813 data points). The raw time-series of DOC measurements shows some anomalous concentration peaks which do not always match a peak in discharge (Figure 1). Peak values for which concentration exceeds 4 mg L^{-1} (n = 5, red points in Figure 1) were removed based on Battin (1999) and Fasching

et al. (2016) previous data pre-processing. For an extensive time window within the sampling period (from January 2011 to the end of August 2013, see blue box in Figure 1), the fluorescence EEMs and the absorbance spectra were also measured for each DOC sample. These data allowed computing a suite of metrics useful to characterize DOC quality and composition (see Section 2.2).

Regarding hydrology and climate, streamflow discharge was measured at a 30-min interval (with some periods at a finer, i.e. 10-minute, interval) from 15 July 2010 to 31 August 2013 (132,396 observations). Rainfall and air temperature were recorded by the Zentralanstalt für Meteorologie und Geodynamik (ZAMG) at the nearby Lunz am See meteorological station (see Figure 1) at 10-min interval (192,454 observations spanning the same DOC sampling period). Across the study period, discharge ranged between 0.003 and 4.041 mm h^{-1}, with the most abundant regimes observed in spring (average flow = 0.29 mm h^{-1}) and the lowest in winter (average flow = 0.13 mm h^{-1}). Precipitation peaks during spring and summer storms (maximum intensity recorded over the sampling interval = 90 mm h^{-1}). Rainfall patterns show an annual increase from the winter minimum to summer maximum, followed by a consequent decrease during autumn. In the same period, air temperature varied between −23 and +35 °C, with the annual maximum typically observed in July and the annual minimum occurring between December and February. Additional details about hydrology, water quality and climate data used in this study are exposed extensively in Fasching et al. (2016).

2.2. Assessing DOC Quality

Assessing riverine DOC quality involves depicting its sources, composition, and transformations as it flows through the watershed and the river network. To achieve these goals, fluorescence and absorbance analysis are commonly performed; the previous to measure emissions following excitation of DOC at specific wavelengths, the latter to assess how much light a sample absorbs at specific wavelengths (see e.g., Baker & Spencer, 2004; Korak & McKay, 2024, for a comprehensive review). Excitation Emission Matrices (EEMs) provide a 3D map of fluorescence, capturing excitation and emission spectra. The location of fluorescence peaks in each EEMs indicates the presence of specific DOC characteristics: humic-like substances suggest terrestrial or soil-derived molecules, while protein-like substances indicate microbial or algal activity, likely to be originated in-stream. On the other hand, absorbance spectra are used to assess, through the calculation of specific indexes, DOC aromaticity (referring to the presence and abundance of aromatic compounds, indicating terrestrial inputs) and molecular size (smaller molecules are typically more bioavailable, while larger, humic-like molecules are less reactive).

The fluorescence data set collected by Fasching et al. (2016) included EEMs ranging 240–450 nm (5-nm increments) for Excitation (Ex) wavelengths and 250–550 nm (2-nm increments) for the Emission (Em) wavelengths. EEMs were expressed in Raman units, corrected for Milli-Q water blanks and the inner-filter effects using the absorbance spectra. After inspecting them, we corrected each EEM for the 1st and 2nd order Raman scatter and 1st order Rayleigh scatter (see Supplementary Information, SI, for additional details).

Within the MATLAB environment, we used the drEEM toolbox v.0.6.0 (Murphy et al., 2013) (embedding the N-way toolbox v.3.3.1) to perform a Parallel Factor Analysis (PARAFAC) on the sampled EEMs according to Murphy et al. (2013) (see Supporting Information SI for details). Fluorescence PARAFAC is a way to decompose multi-way data, such as the EEMs, into a set of scores and loads which provide information about the underlying fluorophores. The analysis results in a set of components representative of the dataset and their temporal contribution to the total fluorescence. This type of analysis is therefore widely applied in chemometrics to unravel the key features of aquatic DOC samples such as their origin or degree of processing (Bro, 1997; Kothawala et al., 2014; Murphy et al., 2013, 2014). In order to further validate and characterize the set of components obtained, we compared them with matching spectra in the OpenFluor data base (https://openfluor.lablicate.com/; accessed 20 September 2022). Moreover, we used the drEEM toolbox to compute two indexes that are good indicators of the source and aromaticity of DOC moieties: the Humification Index (HIX, Zsolnay et al., 1999) from the EEMs to assess DOC degree of humification; and the $SUVA_{254}$ index from the absorbance spectra as a measure of aromaticity (Weishaar et al., 2003). High values for these two indexes reveal high degree of humification and aromaticity and are thus associated to fresh terrestrial DOC. The set of components identified via the PARAFAC analysis, together with the HIX and $SUVA_{254}$ indexes can be used to track temporal dynamics of DOC quality, and to assess its behavior under different hydrologic conditions. Specifically, we investigated DOC quality signature under three distinctive hydrologic regimes of interest for an alpine catchment (as shown in Figure 2): snowmelt,

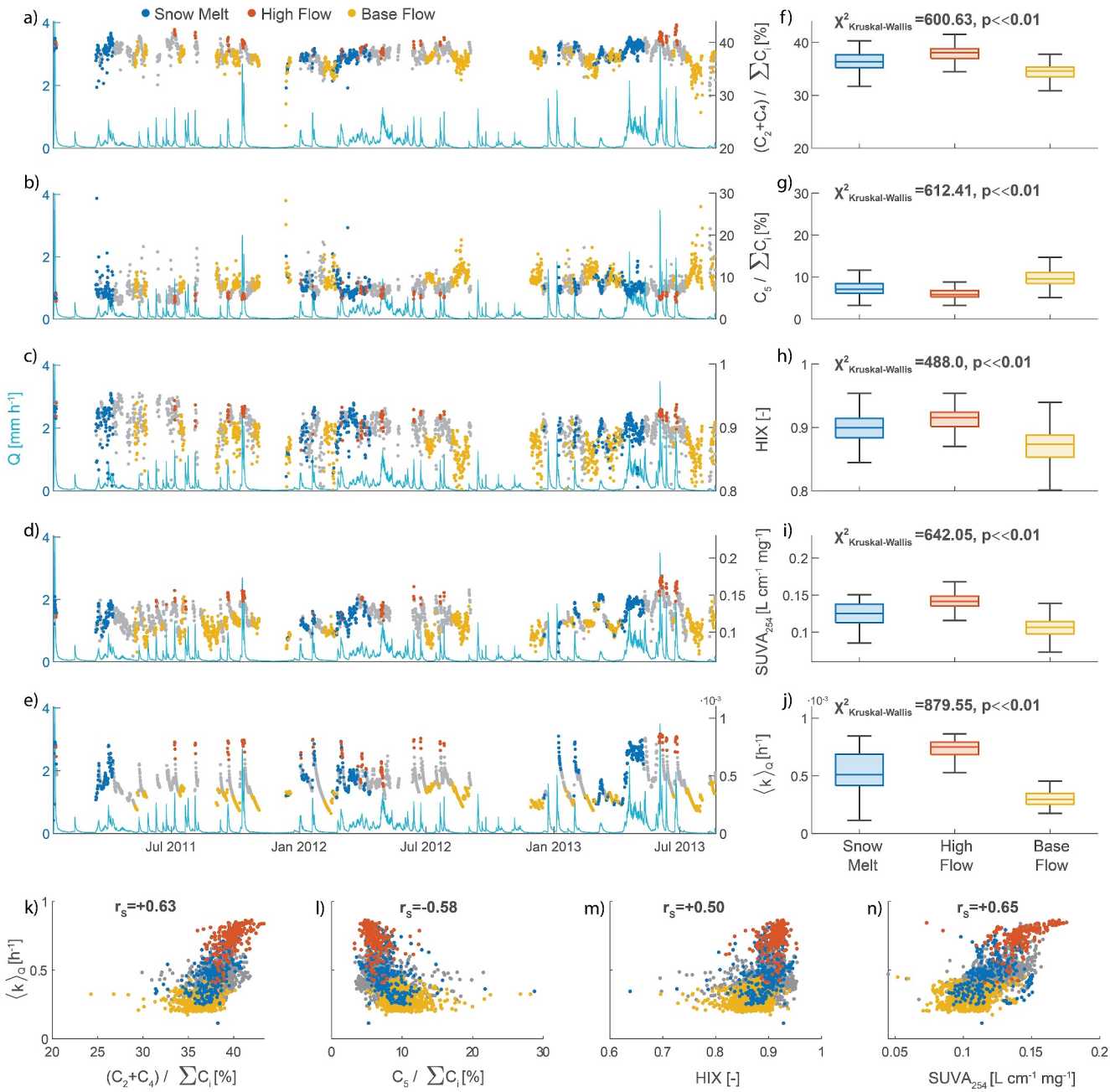

Figure 2. (a)–(e) Time series of the quality indexes obtained from the EEMs and the absorbance spectra and the predicted average reactivity $\langle k \rangle_Q$ (dots). Discharge Q time series is also shown in light blue. (a) Relative abundance of the sum of the PARAFAC components C_2 and C_4 and (b) relative abundance of the PARAFAC components C_5. Time series of the 5 PARAFAC components can be found in the SI. (c) Humification (HIX) and (d) $SUVA_{254}$ index, (e) $\langle k \rangle_Q$. Time series are colored according to three different flow regimes: snowmelt (403 data-points, blue dots), storms (226 data-points, orange dots) and baseflow (723 data-points, yellow dots). (f)–(j) Distribution of indexes values under the three selected flow conditions. For each index, we tested the similarity of the three flow classes selected through the Kruskal–Wallis test. p-Values obtained where always lower than 10^{-105}. (k–n) correlations between $\langle k \rangle_Q$ and (k) the relative abundance of the sum of the PARAFAC components C_2 and C_4 and (l) the relative abundance of C_5 over the total components (in %), (m) HIX, and (n) $SUVA_{254}$. For each relation the Spearman's rank correlation coefficient r_S is also displayed on top of the panels.

discharge data points in which the model (see Section 2.4) predicts a snowmelt contribution to discharge, storms: high-discharge events when snowmelt is not occurring, and baseflow, low discharge not occurring during snowmelt. We set thresholds of 0.45 mm h^{-1} and 0.05 mm h^{-1} to discriminate high and low discharge, corresponding to the 90^{th} and 30^{th} percentile of the cumulative flow distribution observed within the study period, respectively.

2.3. Modeling DOC Concentration and Reactivity

For the paper to be self-contained, this Section starts summarizing the modeling framework that couples water TTD with the RC model to describe DOC export and degradation, as introduced in Grandi and Bertuzzo (2022). The model assumes that water gets enriched in DOC while infiltrating through the superficial C-rich soil layers. This DOC is then progressively degraded along the flowpath that connects the source to the stream. The degradation process is modeled via the RC model, which assumes that DOC is a complex mixture of molecules characterized by different reactivity rates. Mathematically, DOC composition is described by a continuous distribution of reactivity rates (i.e., first order decay rates). The time available for DOC degradation is dictated by the transit time of water.

Central to the model is the definition of the density $\rho(k,T,t)$, which describes the distribution of age T (i.e., the time elapsed since the water entered the system) and reactivity k of the DOC within the catchment considered. Specifically, $\rho(k,T,t)dkdT$ represents the mass of DOC of reactivity in an infinitesimal interval dk around k transported by water parcels with a residence time around T at time t. The governing equation for $\rho(k,T,t)$ reads:

$$\frac{\partial \rho(k,T,t)}{\partial t} + \frac{\partial \rho(k,T,t)}{\partial T} = -k\,\rho(k,T,t) - \frac{p_Q(T,t)Q(t)}{s(T,t)}\rho(k,T,t), \tag{1}$$

with the boundary condition that the water parcels entering the system as input $I(t)$ have $T = 0$ and carry an initial DOC concentration with a distribution of reactivity $C_0(k,t)$ so that $\rho(k,T = 0,t) = C_0(k,t)I(t)$. The second term of the left-hand side of Equation 1 describes aging, while the first term of the right-hand side models degradation, where each DOC fraction degrades following a linear decay equation according to its reactivity k. The last term of Equation 1 represents the export of $\rho(k,T,t)$ from the catchment associated to the discharge flux $Q(t)$; and $s(T,t)dT$ quantifies the catchment storage of water of age around T at time t. The export flux crucially depends on the transit time distribution (TTD) of the discharge $p_Q(T,t)$, where $p_Q(T,t)dT$ quantifies the probability that discharge at time t samples water with an age around T. We thus implemented the StorAge Selection (SAS) scheme (Benettin & Bertuzzo, 2018; Benettin et al., 2022; Rinaldo et al., 2015) to describe in a consistent way time-variable transit time distributions. The scheme revolves around the definition of the age-ranked storage $S_T(T,t)$, namely the volume of water stored in the system younger than age T at a given time t, whose governing equation reads (see e.g., Harman, 2015; Rinaldo et al., 2015; van der Velde et al., 2014):

$$\frac{\partial S_T(T,t)}{\partial t} + \frac{\partial S_T(T,t)}{\partial T} = -Q(t)\Omega_Q(S_T(T,t),t) + I(t). \tag{2}$$

Analogously to Equation 1, the second term on the left-hand side represents the variation of S_T due to aging; while the first term on the right-hand side represents the output through discharge weighted by the SAS function $\Omega_Q(S_T(T,t),t)$: the fraction of $Q(t)$ that is younger than T. To solve for Equation 2, and in turn for the coupled Equation 1, one needs to choose a specific form for the SAS function, here expressed in terms of S_T (see below). Finally, the estimation of the TTD p_Q follows by definition from the identities $\Omega_Q(S_T(T,t),t) = P_Q(T,t)$, where P_Q represents the cumulative distribution of p_Q. Transit time refers to the age T of water particles collected at a specific cross-section, such as the catchment outlet, where discharge is measured or estimated. The transit time typically comprises two periods: the time spent within the soil and the time spent in the streamflow. Given the size of the OSB catchment, it is reasonable to assume that the time spent in the stream is negligible compared to the time spent in the soil. Therefore, transit time can effectively be considered equivalent to the time water spends in the soil. Correspondingly, the associated DOC degradation processes can also be regarded as those occurring within the soil.

Similarly, DOC collected at a stream cross-section can consist of molecules originating from the soil (allochthonous DOC) as well as from the upstream portion of the stream network (autochthonous DOC). Given the relatively small size of the catchment and the previous knowledge of the site (i.e., strong terrestrial signature of DOC and relatively low in stream metabolic activity, Fasching et al., 2016; Ulseth et al., 2018), we hypothesize that DOC is primarily dominated by soil sources. Therefore, our modeling focuses on the transport and reaction of allochthonous DOC. This hypothesis will be tested through the analysis of the PARAFAC results.

Table 1
List of Fixed Parameters

Parameter	Symbol	Units	Value
Snow threshold temperature	$\mathcal{T}_S$	°C	0
melting threshold temperature	$\mathcal{T}_M$	°C	1
Degree-day factor	α_S	mm h^{-1} $°C^{-1}$	0.14
Storage-discharge relation exponent	b	–	1

2.4. Model Development and Application

This Section presents further model developments that provide higher model flexibility and facilitate the application to this specific case study. Due to the alpine climate of the OSB catchment, we further accounted for snow dynamics, which strongly affect hydrologic processes during winter and spring. Precipitation J can occur as snow precipitation (J_S) or rainfall (J_R) based on an air temperature ($\mathcal{T}(t)$) threshold $\mathcal{T}_S$. We then adopted a simple degree-day approach (Rango & Martinec, 1995) to model snowpack (h_s) dynamics: $dh_s/dt = J_S(t) - J_M(t)$, where snowmelt $J_M(t)$ linearly depends on air temperature: $J_M(t) = \alpha_S(\mathcal{T}(t) - \mathcal{T}_M)$ when $\mathcal{T}(t) > \mathcal{T}_M$ and $h_s(t) > 0$, and it is null otherwise. The three parameters related to snow dynamics ($\mathcal{T}_S$, $\mathcal{T}_M$ and α_S) were retrieved from a previous application of the degree-day model on the same catchment (Ulseth et al., 2018, Table 1). The total input of water to the catchment control volume is then $I(t) = J_R(t) + J_M(t)$, while storage $S(t)$ can be computed as $S(t) = S_0 + \int_0^t (I(\tau) - Q(\tau))d\tau$ where S_0 is the volume stored at the beginning of the simulation and the observed discharge $Q(t)$ is used. As in Grandi and Bertuzzo (2022), we did not explicitly consider evapotranspiration, but rather rescaled rainfall so that it implicitly accounts for it. Specifically, we rescaled rainfall so that the average rainfall equals the average specific discharge: $\langle J \rangle = \langle Q \rangle$. Rescaling rainfall to model evapotranspiration implicitly assumes that this flux preferentially selects young water. While this is an approximation, it is deemed acceptable for a catchment with a low fraction of evapotranspiration in the water budget (around 10% during the selected period).

We chose a time-variant (see e.g., Benettin et al., 2017; Harman, 2015) power-law SAS function of the form

$$\Omega_Q(S_T, t) = \left[\frac{S_T(T,t)}{S(t)}\right]^{\beta(t)}, \tag{3}$$

where the exponent β, which quantifies the preference for discharge to sample young ($\beta < 1$) or old ($\beta > 1$) water in storage, is assumed to possibly vary in time to reflect how different hydrologic states of the systems can activate different flowpaths. As in several previous applications (see e.g., Harman, 2015), we assumed that β is related to the system storage. Rather than considering the total storage $S(t)$, which can exhibit large intra- and inter-annual fluctuations, we related β to a dynamical storage $S_d(t)$ (Harman, 2015) more directly related to streamflow generation processes, via a linear function: $\beta(t) = \beta_1 + \beta_2 S_d(t)$. We reconstruct S_d via a storage-discharge relationship (Botter et al., 2009; Brutsaert & Nieber, 1977; Kirchner, 2009): $Q(t) \propto S_d(t)^b$ (i.e.,: $S_d(t) = aQ(t)^n$, $n = b^{-1}$). The exponent b can be estimated through a flow recession analysis (Brutsaert & Nieber, 1977), which yielded $b \approx 1$ for the OSB (see Text S3 and Figure S5 in Supporting Information S1). Note that the parameter a does not need to be explicitly estimated as it can be embedded into the parameter β_2. We evaluated the young water fraction, F_{yw}, as a summary statistic for the TTD (Kirchner, 2016). F_{yw} represents the fraction of discharge water younger than a threshold age, T_{yw}: $F_{yw}(t) = P_Q(T_{yw})$, which was set to 2 months.

Grandi and Bertuzzo (2022) used a gamma distribution as initial DOC reactivity distribution as it allows deriving an analytical solution for the quantity $C(T,t)$, that is, the DOC concentration carried by water of age T at time t. However, being tied to a specific distribution limits the array of possible initial distributions that can be tested. In this paper we propose to use a linear combination of gamma distributions which enables more flexibility (including e.g. multimodal distributions), while preserving analytical tractability:

$$C_0(k,t) = \sum_{i=1}^{n} D_{0,i}(t) \frac{\alpha_i^{\nu_i}}{\Gamma(\nu_i)} k^{\nu_i - 1} e^{-\alpha_i k} \tag{4}$$

where $\Gamma(\cdot)$ is the gamma function and the coefficients $D_{0,i}(t)$ represent the, possibly time variant, initial DOC concentration associated to the i-th distribution. ν_i and α_i are the shape and the scale parameters of the distribution, respectively.

DOC concentration in the exported discharge $C_Q(t)$ in the case of a combination of gamma distributions reads:

Table 2
List of Estimated Parameters and Posterior Statistics

Parameter	Symbol	Units	Limits	Estimated median value (95% C.I.)	
				Distribution 1	Distribution 2
Parameter of the relation $\beta(t) = \beta_1 + \beta_2 \cdot S_d(t)$	β_1	–	0–2	0.384 (0.364–0.406)	
Parameter of the relation $\beta(t) = \beta_1 + \beta_2 \cdot S_d(t)$	β_2	mm^{-1}	−0.5–0	−0.249 (−0.282–−0.221)	
Initial volume of water in storage	S_0	mm	0–30,000	22,452 (14,828–29,633)	
Mean of the initial DOC quality distribution	$\langle k \rangle_i$	h^{-1}	0–0.2	0.1015 (0.0057–0.1945)	0.0012 (0.0010–0.0014)
Shape of the initial DOC quality distribution	ν_i	-	0–10	0.0013 (0.00003–0.0104)	8.777 (4.972–9.9630)
Initial DOC concentration for each distribution	$D_{0,i}$	mg l^{-1}	0–10	0.40 (0.19–0.59)	5.30 (4.80–5.76)
Concentration of DOC in the initial storage	$C_{S_0,i}$	mg/l	0–5	1.24 (1.17–1.35)	0.25 (0.11–0.37)
Standard deviation of the DOC concentration residuals	σ_ϵ	mg/l	0.1–5	0.206 (0.201–0.212)	

Note. For each parameter the range for sampling and the resulting median value and 95% percentile range are displayed. The results for the standard deviation of the concentration residuals σ_ϵ are also shown.

$$
\begin{aligned}
C_Q(t) &= \int_0^\infty p_Q(T,t)C(T,t)dT = \int_0^\infty p_Q(T,t)\left[\int_0^\infty C_0(k,t-T)e^{-kT}dk\right]dT = \\
&= \int_0^\infty p_Q(T,t)\left[\sum_{i=1}^{n} D_{0,i}(t-T)\int_0^\infty \frac{\alpha_i^{\nu_i}}{\Gamma(\nu_i)}k^{\nu_i-1}e^{-(\alpha_i+T)k}dk\right]dT = \\
&= \int_0^\infty p_Q(T,t)\left[\sum_{i=1}^{n} D_{0,i}(t-T)\left(\frac{\alpha_i}{\alpha_i+T}\right)^{\nu_i}\right]dT
\end{aligned}
\tag{5}
$$

Finally, we derived the average reactivity of the exported DOC, $\langle k \rangle_Q$, as:

$$
\begin{aligned}
\langle k \rangle_Q(t) &= \frac{1}{C_Q(t)}\int_0^\infty p_Q(T,t)\left[\int_0^\infty k\, C_0(k,t-T)e^{-kT}dk\right]dT = \\
&= \frac{1}{C_Q(t)}\int_0^\infty p_Q(T,t)\left[\sum_{i=1}^{n} D_{0,i}(t-T)\int_0^\infty \frac{\alpha_i^{\nu_i}}{\Gamma(\nu_i)}k^{\nu_i}e^{-(\alpha_i+T)k}dk\right]dT \\
&= \frac{1}{C_Q(t)}\int_0^\infty p_Q(T,t)\left[\sum_{i=1}^{n} D_{0,i}(t-T)\frac{\nu_i\alpha_i^{\nu_i}}{(\alpha_i+T)^{\nu_i+1}}\right]dT
\end{aligned}
\tag{6}
$$

The mathematical expression of Equation 6 allows for a computationally efficient scheme for the estimation of the modeled average reactivity and for comparison with different DOC quality metrics that can be associated with its reactivity. Note that the calculation of p_Q and the integration over T must be performed numerically as detailed in Grandi and Bertuzzo (2022). In this first application, we set $n = 2$ in order to limit the number of parameters to be estimated yet allowing some flexibility in the definition of the initial distribution of reactivity. We did not assume any a priori knowledge on the two gamma distributions, but we set the same range for the estimation of their parameters (Table 2). We estimated parameters in terms of the mean reactivity of the gamma distribution: $\langle k \rangle_i = \nu_i/\alpha_i$, rather than the scale parameter α_i, in order to facilitate the interpretation of the resulting values. A temperature dependent function can be used to account for the possible seasonality of the input DOC concentration (Grandi & Bertuzzo, 2022). However, stream DOC concentration in the OSB does not exhibit a clear seasonal fluctuation; and in the first trials that included such function, posterior distribution converged to values indicating no temperature effect. For model parsimony, we therefore decided to neglect temperature dependence (i.e., $D_{0,i}(t) = D_{0,i}$).

2.5. Parameter Estimation

The model estimated a total of 11 parameters (Table 2): 3 for the definition of the water age dynamics (β_1, β_2 and S_0), and 6 for the description of the initial DOC reactivity, including 3 parameters for each of the $n = 2$ initial reactivity distributions that describe the shape of the gamma distribution ($\langle k \rangle_i$ and ν_i) and the initial DOC

concentration $D_{0,i}$. Finally, the concentration of DOC $C_{S_0,i}$ of the initial storage S_0 is also estimated to define the initial conditions. Parameter estimation was performed in a Bayesian framework assuming uninformative uniform prior distributions (within the limits shown in Table 2) and independent, identically distributed normal errors with standard deviations σ_ϵ between the observed and simulated DOC concentration time series $C_Q(t)$. We sampled the parameter posterior distribution using the DREAM$_{ZS}$ (ter Braak & Vrugt, 2008; Vrugt et al., 2009) implementation of the Markov Chain Monte Carlo algorithm.

The model was implemented using a 6-hr time-step since this is the interval at which all the variables were simultaneously sampled. We did not explicitly include information on DOC quality in the likelihood calculation. Rather, based on the best performing parameter set, we computed *a-posteriori* the correlation between the average reactivity simulated by the model $\langle k \rangle_Q$ and the DOC quality metrics (i.e., PARAFAC components, SUVA$_{254}$, and HIX). As we did not expect a linear relation between DOC reactivity and DOC quality metrics, we quantified the correlation using the Spearman's rank correlation coefficient. It is worth emphasizing that tracers observations were not available to independently estimate the SAS function parameters. We thus estimated both the SAS and the initial reactivity distribution parameters solely reproducing DOC concentration in the discharge.

3. Results

3.1. DOC Quality

The PARAFAC analysis revealed the presence of 5 components (C_1-C_5), 4 humic-like and 1 protein-like associated with in-stream production. C_1 (Ex: 240 (310)/Em: 415), is assigned to a terrestrial humic-like character, linked with microbial processing and biological activity (Gao & Guéguen, 2017; Murphy et al., 2014) (20 models had coincident components in OpenFluor). C_2 (Ex: 240 (425)/Em: 488), previously related with peatlands (Galletti et al., 2019; Yamashita et al., 2011), provides a strong terrestrial signature (2 models matched in OpenFluor). C_3 (Ex: 330/Em: 438) showed a similar signature to marine peak M (Coble, 1996), terrestrial humic-like with some degree of microbial processing (Gao & Guéguen, 2017; Kauai; 6 models matched in OpenFluor). C_4 (Ex: 240 (370)/Em: 462), related to a terrestrial-humic component (Gao & Guéguen, 2017), has been found previously in mountain streams (Yamashita et al., 2021) and matched 4 models in OpenFluor. C_5 (Ex: 280/Em: 330) is a protein-like component (Cawley et al., 2012; Wünsch & Murphy, 2021), likely produced instream, and characterized by high reprocessing rates (Kothawala et al., 2014), 14 models matched in OpenFluor. All spectra with combined Tuker Congruent Coefficient (TCC) for excitation and emission > 0.95 were considered similar, except for C_2 for which TCC threshold was set to > 0.94. These PARAFAC components mostly agree with those identified by Fasching et al. (2016) (see Supporting Information SI). These results confirm our initial working hypothesis that stream DOC in the OSB is dominated by terrestrial components. Indeed, the only protein-like component, C_5, with an autochthonous origin, contributed to a small extent to stream DOC (typically <9% with few peaks at 15%), acting as an almost constant baseline (see Figure S3 in Supporting Information S1). This finding suggests a minimal contribution of in-stream production to the stream's DOC concentration, which allows for a direct comparison between the model results—focused solely on the transport and degradation of terrestrial DOC—and the data collected from the stream. Components C_2 and C_4, which together accounted for 30%–40% of the total fluorescence (Figure 2, panel a), are of particular interest for the purpose of this study because they represent the humic, terrestrial signature of the system. Among the 5 components, these are most strongly linked to the fresh terrestrial DOC. These components are characterized by lower degree of processing in comparison to C_1 and C_3. Based on these results, we computed an additional quality index to quantify the relative contributions of components 2 and 4 to the total DOC mixture: $(C_2 + C_4)/\sum C_i$. High values of this index indicate the presence of fresh terrestrial DOC that has undergone limited degradation processes. In contrast, low values imply a stronger contribution from components 1 and 3, suggesting a DOC mixture with a higher degree of processing. Therefore, according to the hypothesis presented in the Introduction, we expect fast hydrological pathways to be characterized by high values, and slow pathways by low values, of the relative contribution of components 2 and 4.

The DOC collected in the OSB catchment shows clear, distinct quality signatures across different hydrologic conditions. As conditions shift from baseflow to snowmelt and peak flows, we observed statistically significant increases in HIX, SUVA$_{254}$, and the relative contribution of the combined PARAFAC components C_2 and C_4. Conversely, the relative contribution of component C_5 decreases with increasing flow conditions (Figures 2a–2d, 2f–2i).

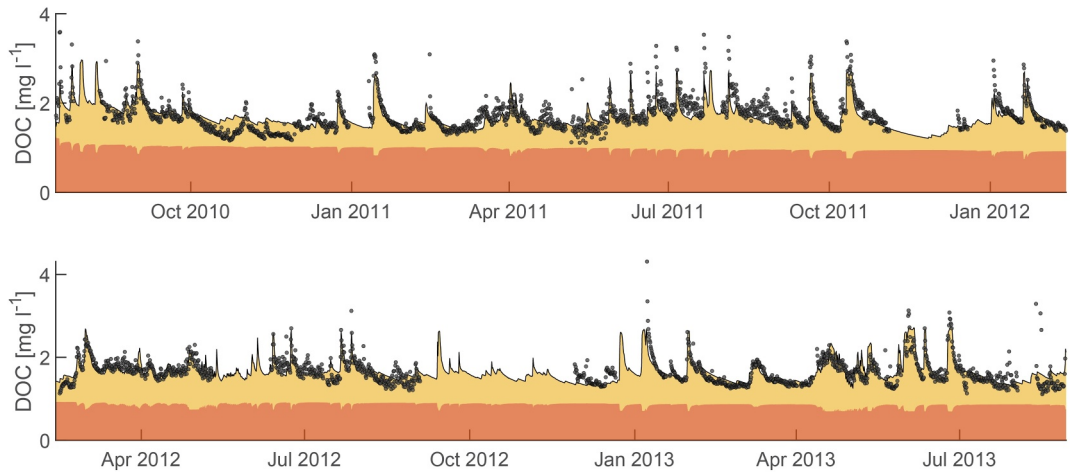

Figure 3. Observed (dots) and simulated (black line) DOC riverine concentration time series in the OSB river. The contribution to total DOC concentration of the two different fractions characterized by different initial reactivity distributions is also shown: the orange area represents the contribution of the recalcitrant DOC composing the first reactivity distribution and the yellow area represents the contribution of the second distribution, comprising more reactive DOC. Note that the study period is split in two to enhance representation: from 17 May 2010 to 13 February 2012 (top panel), and from 13 February 2012 to 31 August 2013 (bottom panel).

3.2. Simulated DOC Concentration

The model is able to reproduce the temporal fluctuations of stream DOC concentration (Figure 3), including its response to precipitation and snowmelt that typically occur in April (see Figure 2). Stream DOC exhibits a typical flushing behavior (Stewart et al., 2022), with concentrations increasing with increasing discharge. While some peaks in DOC concentration were not correctly reproduced (e.g., during summer 2011), the overall model performance was satisfactory, reaching a Nash-Sutcliffe coefficient of 0.62 (root mean square error = 0.21 mg L^{-1}).

The analysis of the parameter posterior distribution (Figure 4 and Table 2) sheds further light on the processes governing stream DOC concentration. With respect to the SAS function, a negative value for the parameter β_2 indicates that, as the storage increases, $\beta(t)$ decreases and discharge is more prone to select younger water particles in the storage. Overall the mean value of $\beta(t)$ is 0.34 indicating a strong preference for young water. The initial storage S_0 resulted in a large median estimated value of $\approx$ 22000 mm. In this case, the posterior distribution was not well defined with all the values greater than 22,000 mm showing a similar probability. This is a common drawback of this type of analysis, especially when the system has a strong preference for young water (see e.g. Benettin et al., 2017; Hrachowitz et al., 2015, 2021).

With respect to stream DOC dynamics, the two estimated gamma distributions (D_i) that constitute the initial DOC reactivity spectrum exhibit markedly different characteristics: a persistent compartment with very low reactivity ($i = 1$) and a more labile, reactive, compartment ($i = 2$). The relative contribution of these two distributions to simulated stream DOC concentration fluctuates over time (Figure 3). The persistent DOC attributed to the initial distribution D_1 contributed to a basal, almost stable DOC concentration of around 1.2 mg L^{-1}; while the contribution of the reactive DOC was highly variable over time (from around 0 to 3 mg L^{-1}) and increased during storm events and snowmelt periods (Figure 3, yellow area). Parameter-wise, D_1 resulted in a shape factor ν_1 that tended to zero, which means that the distribution tends to an atom of probability in $k = 0$. With such low values of ν_1, the soil DOC fraction characterized by this distribution has an almost non-reactive behavior regardless of the mean reactivity $\langle k \rangle_1$. Consequently, $\langle k \rangle_1$ showed a uniform posterior distribution of values (Figure 4). Conversely, D_2 is characterized by a relatively fast mean reactivity (median $\langle k \rangle_2 = 0.0013$ h^{-1}) and a larger shape factor (median value $\nu_2 = 8.78$), which lead to a mound-shaped distribution. We note that as ν increases, a gamma distribution tends toward a Gaussian distribution. Therefore, even though the posterior distribution of ν_2 is squeezed toward the defined upper boundary ($\nu_2 = 10$), we do not deem necessary to increase the upper bound because the shape of the distribution for $\nu_2 > 10$, and a fixed mean value, is almost invariant.

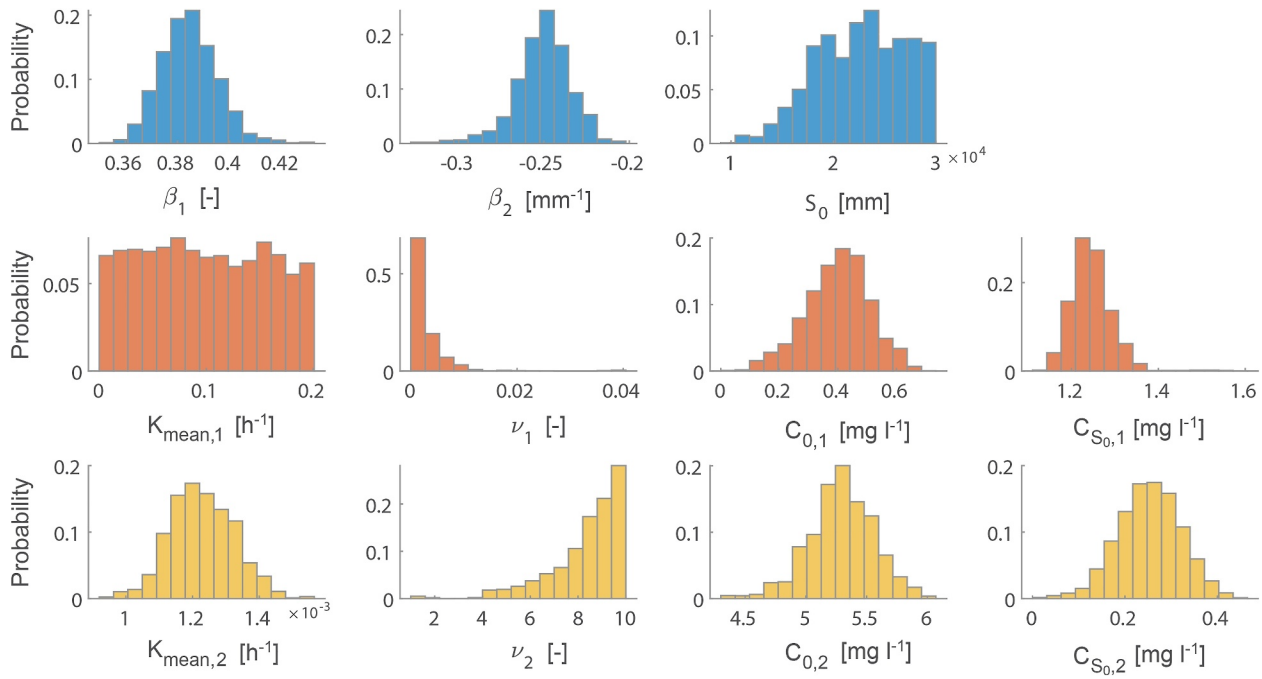

Figure 4. Marginal posterior distributions obtained in a Bayesian framework for the 3 parameters related to the time-variant SAS function (top panels, blue) and for the two initial DOC gamma reactivity distributions in soil (middle and bottom panels, in orange and yellow for the first and second gamma reactivity distribution, respectively).

3.3. Simulated DOC Reactivity

The average DOC reactivity $\langle k \rangle_Q$ predicted by the model via Equation 6 is showed in Figure 2e. Under the three different hydrologic regimes considered, $\langle k \rangle_Q$ exhibit the same behavior of the quality indexes HIX, $SUVA_{254}$ and $(C_2 + C_4)/\sum C_i$, exhibiting an higher median value of $7.50 \cdot 10^{-4}$ h^{-1} at high flow, versus $5.11 \cdot 10^{-4}$ h^{-1} during snowmelt and, $2.96 \cdot 10^{-4}$ h^{-1} at baseflow (2e). Moreover, our results prove $\langle k \rangle_Q$ to be positively correlated with HIX (Spearman's rank correlation coefficient $r_S = 0.50$) and $SUVA_{254}$ ($r_S = 0.65$) indexes, albeit with a notable dispersion. Moreover, we find $\langle k \rangle_Q$ to be positively related with the relative contribution of the sum of C_2 and C_4 to the overall fluorescence (Figures 2k–2n). In contrast, $\langle k \rangle_Q$ showed weaker correlations with the relative contribution of C_1 ($r_S = -0.21$) and C_3 ($r_S = +0.28$). Finally, we find a negative correlation (r_S = -0.58) between $\langle k \rangle_Q$ and the relative contribution of C_5.

4. Discussion

Different flow regimes in the OSB catchment export DOC with distinct quality features. The analysis of quality indexes derived from high-resolution EEMs data and absorbance spectra shows that as conditions shift from baseflow to snowmelt to peak flow, the exported DOC is characterized by higher values of the HIX and $SUVA_{254}$ indexes, and shows a greater relative contribution of PARAFAC components C_2 and C_4. This result suggests that peak flow activates pathways that transport fresh terrestrial DOC with a short history of degradation, while DOC exported during baseflow exhibits signatures of longer degradation and processing. Snowmelt is characterized by a wide range of flow magnitudes that lie between baseflow and stormflow, and the quality signature of snowmelt DOC also exhibits characteristics intermediate between these two regimes (Figure 2). When comparing the quality of DOC during snowmelt with that of DOC exported during similar flow magnitudes, no distinctive features were observed (see Figure S4 in Supporting Information S1). This suggests that DOC quality during snowmelt is primarily controlled by the level of flow discharge rather than specific biogeochemical processes occurring during these events.

The relationship between flow regime and DOC quality is further supported by the model results. The framework simulates the evolution of DOC reactivity from its initial distribution, when DOC is exported from superficial soil

10.1029/2024WR039392

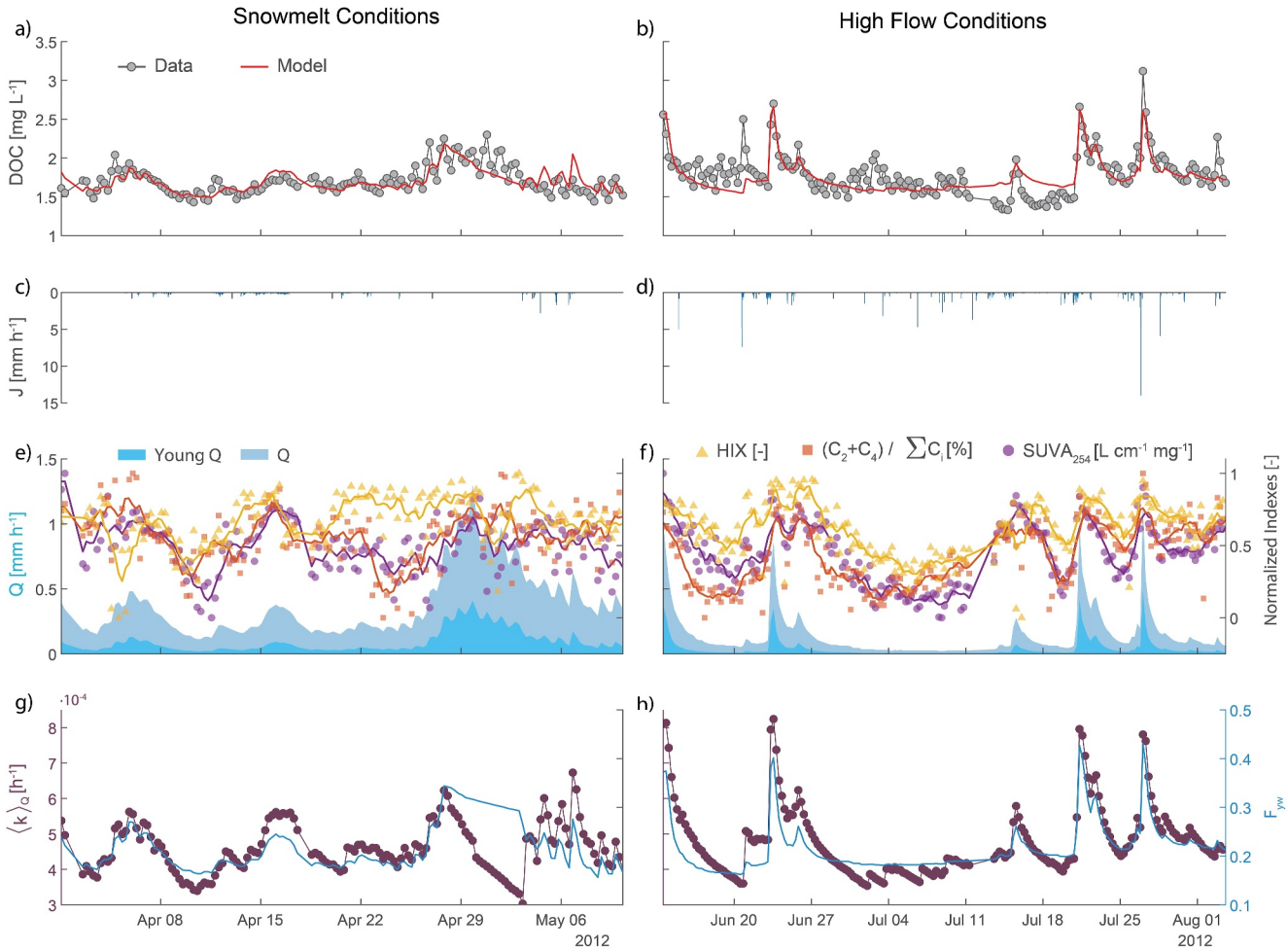

Figure 5. DOC dynamics under different hydrologic conditions: 2012 spring snowmelt (left panels) and 2012 summer high flow (right panels). (a, b) Observed and modeled DOC riverine concentration. (c, d) Observed rainfall. (e, f) Observed discharge Q and estimated young Q mobilized (i.e., the fraction of discharge younger than 2 months) - blue areas, versus the three selected DOC terrestrial indexes (HIX, relative abundance of $C_2 + C_4$ and $SUVA_{254}$ index) normalized to 1. Continuous yellow, orange and purple lines display the corresponding index moving average calculated over a 36-hr time window. (g, h) Comparison between the average reactivity $\langle k \rangle_Q$ (purple dotted line) and the fraction of young water (blue line) estimated by the model.

layers, up to the sampling point. Along the flow pathway, the DOC reactivity distribution is used to compute the time-varying bulk DOC degradation rate, which predicts the quantity of DOC exported from the catchment. Additionally, the predicted reactivity distribution provides relevant information on DOC composition. According to this scheme, DOC molecules with high reactivity are quickly degraded along the flowpath, causing the reactivity distribution to shift toward lower k values. As a result, DOC that is transported for long (short) transit times will have a low (high) mean reactivity at the end of the transport process. From a quality perspective, DOC with a long transit time should exhibit a high degree of processing, while DOC transported via shorter pathways will carry fresh terrestrial material with a shorter history of degradation. This relationship is confirmed when comparing quality indexes with the predicted mean reactivity (Figure 2): predicted mean reactivity is positively correlated with quality indexes that point toward a fresh DOC with low degree of processing (HIX, $SUVA_{254}$, and the relative contribution of PARAFAC components C_2 and C_4). Notably, this correlation was not a specific objective of the model calibration, which was based solely on reproducing DOC concentrations. Instead, it emerged a posteriori, based on the best-performing parameters.

Such system functioning is further detailed in Figure 5 which illustrates how DOC concentration and composition vary in the OSB stream under the three distinct hydrologic conditions considered. In particular, left panels focus on some spring snowmelt events in 2012, whereas right panels analyze the succession of storm and baseflow events observed in summer of the same year. With the occurrence of a storm, the fraction of discharge water

younger than 2 months quickly increases from values of 20%, typical of baseflow, to up to 45% during peak discharge. As a consequence, the presence of water parcels with short transit times leads to an increase of the average DOC reactivity (panel g–h). An analogous response is observed for the quality indexes (panel e–f) that peak during these events. It should be noted that while mean reactivity decreases rapidly after a storm, the quality indices exhibit a more persistent signal. This difference underlies the good, though not perfect, correlation between these variables (Figures 2k–2n). During snowmelt, the young water fraction reaches a maximum value of around 35% (panel g), which is lower than the levels observed during similar discharges caused by isolated storms (panel h). Consequently, the predicted mean reactivity also results to be lower during snowmelt events (panel g). While we found that the quality signature of DOC during snowmelt is not significantly different from that of DOC exported during other periods with similar discharge magnitudes (Figure S4 in Supporting Information S1), it is important to note that the temporal structure of these pulses is entirely different. As discussed in previous work on DOC dynamics under different regimes, we also found that while DOC quality changes rapidly in response to storms (Butturini et al., 2006), snowmelt can result in extended periods—lasting up to a month—during which the DOC quality profile remains distinct from baseflow conditions (Campbell et al., 2014). Therefore, while a storm acts as a brief, impulsive disturbance to the DOC composition feeding the downstream ecosystem, the prolonged change during snowmelt may trigger an adaptive response in the riverine ecosystem. Indeed, a study conducted in the same catchment revealed a positive effect of snowmelt on both ecosystem respiration and primary production (Ulseth et al., 2018). While the former can be directly linked to DOC quality and concentration, the effect on productivity may be related to the delivery of terrestrial nutrients, which follows dynamics similar to DOC. Other studies in alpine catchments shown how snowmelt triggers slow infiltration in soil and a consequent asynchronous release of C to the stream (Boyer et al., 1997, 2000), while during storms terrestrial C is quickly flushed into the streamflow.

In terms of DOC concentration, the results presented here provide further validation of the framework introduced by Grandi and Bertuzzo (2022). The model successfully reproduced stream DOC concentrations in the small alpine OSB catchment, demonstrating that riverine DOC dynamics can be effectively modeled by accounting for both the transit time distribution of water and DOC degradation during its transport through the catchment, as described by the Reactivity Continuum model. Our findings further emphasize the critical role of hydrology in determining DOC concentrations and their variability throughout the year, even in this high-altitude catchment. The estimated mean value of β, lower than 1, indicates a strong preference for young water in the OSB catchment. Moreover, the convergence of β_2 to negative values suggests that as storage increases, there is a stronger activation of fast flowpaths, leading to an increasing fraction of younger water in the discharge (see Figure 5). This phenomenon, known as the inverse storage effect (*sensu* Harman, 2015), is commonly observed in small headwater catchments (e.g., Benettin et al., 2017; Harman, 2015). We estimated a significantly high value for the initial volume of water stored in the system S_0. Such potential issue has been addressed in several recent studies (see e.g., Benettin et al., 2017; Harman, 2015; Hrachowitz et al., 2021) and the main impacts on solute transport modeling have been discussed in details in Grandi and Bertuzzo (2022). In that study, a sensitivity analysis on the S_0 parameter was carried out, showing that the initial volume of water in the system can be constrained by adding prior information in the estimation process. However, the analysis also showed that different S_0 estimates had little to no impact on simulated solute concentration, confirming that S_0 is noncritical for solute dynamics in catchments with a strong preference for young water. Finally, while the model was able to reproduce the general fluctuations in observed stream DOC concentrations, it should be noted that it did not fully capture the amplitude of extreme highs and lows (Figure 3).

We introduced a new feature to represent the initial reactivity distribution of DOC in soil: a linear combination of multiple gamma distributions. This approach enhances model flexibility while preserving analytical tractability. We limited the model to two distributions to prevent overfitting. Results indicate that the initial DOC reactivity can be effectively captured by the sum of two distinct distributions: (a) a nearly recalcitrant portion ($\nu \to 0$, with low and constant k), which behaves almost as a conservative tracer, and (b) a more reactive portion that undergoes degradation along the flowpath. While the reactive portion is estimated to be more abundant than the recalcitrant one in the superficial soil layer (Table 2), they are instead comparable at the outlet as a result of the degradation of the reactive portion within the soil (Figure 3). During baseflow, the DOC concentration at the outlet is mostly composed by the recalcitrant portion, while snowmelt and storm activate short pathways that carry reactive DOC that underwent low degradation. In this case study, the initial soil DOC reactivity distribution has been estimated through inverse modeling based on DOC measurements in streamwater. While the available data for the OSB

catchment do not allow for independent validation, it is theoretically possible to estimate these quantities by analyzing the reactivity of soil leachate (see, e.g., Chen & Jaffé, 2014). Future applications could thus exploit parallel soil and streamflow water sampling campaigns.

While the PARAFAC components and reactivity distributions describe different aspects of the DOC mixture, our results suggest a potential parallel between the two. Fresh components from terrestrial sources (C_2 and C_4) could be reactive and subject to microbial degradation (Kalbitz et al., 2000), thus tentatively aligning with the more labile portion of the reactivity distributions. Indeed, the relative contribution of these two components (2 and 4) to the total terrestrial DOC (components 1 to 4) is positively correlated with the relative contribution of the labile fraction in the DOC measured at the outlet ($r_S = 0.41$). Furthermore, their average relative contributions are quite similar (0.41 for the relative abundance of PARAFAC component 2 and 4 vs. 0.44 for the reactivity distribution). Conversely, DOC exhibiting evidence of prior microbial degradation (PARAFAC components 1 and 3) may contain byproducts with lower lability, aligning with the recalcitrant portion of the reactivity distribution. Note that the resulting correlation is 0.41 also in this case, as both pairs of variables complement each other to unity. However, attributing two distinct subsets of the PARAFAC components to the two reactivity distributions should be approached with caution, as cross-attributions are both possible and likely. For example, fresh DOC from terrestrial sources may exhibit recalcitrant behavior even before microbial processing and could therefore align with the recalcitrant portion of the reactivity distribution. Similarly, DOC that has already undergone microbial processing might still retain a reactive nature, placing it within the labile portion of the distribution. Finally, PARAFAC component 5 can be attributed to instream production.

Combining the results about DOC concentration, quality and reactivity, the emerging picture of the catchment functioning regulating water chemistry is as follows: precipitation and snowmelt increases water storage and activate fast flow-paths connecting superficial soil layers to the stream. Such flowpaths carry higher concentration of DOC thus leading to the typical flushing behavior (positive correlation between DOC concentration and streamflow discharge) already observed in other catchments (see e.g. Grandi & Bertuzzo, 2022; Stewart et al., 2022) and frequently assumed when modeling carbon fluxes from the terrestrial to the stream ecosystem (Segatto et al., 2023; Wei et al., 2024). Our study shows that not only this pulses are characterized by a higher DOC concentration, they are also more reactive and transport fresher terrestrial DOC. Terrestrial DOC inputs can largely contribute to changes in riverine DOC concentration and quality and this source represents a fresh input of organic matter that could be rapidly degraded and respired by the stream microbial community (Lupon et al., 2019; Marín-Spiotta et al., 2014; Ward et al., 2013). Indeed, previous studies highlighted that the reactivity of allochthonous DOC sources can be even higher than that of autochthonous sources in both lakes (Catalán et al., 2013) and small headwater streams (Fasching et al., 2014). According to our findings, the majority of this terrestrial DOC is likely to be exported to the stream during storms and high-discharge events when young water parcels are mobilized, resulting in fresh, terrestrial DOM, readily available for stream metabolism. It should be noted, however, that the reactivity estimated in our framework reflects degradation processes occurring within the soil. Once DOC enters the stream, its reactivity profile may change. In fact, Berggren et al. (2022) emphasized that DOC reactivity is not solely dependent on the chemical properties of the DOC molecules, but on both these intrinsic characteristics and extrinsic controls, such as the environmental conditions where degradation occurs. Catalán et al. (2021) proposed a transformation to the reactivity distribution to account for varying environmental conditions. While this method was originally applied to model the different degradation conditions of particulate organic carbon in wet versus dry streambeds, a similar approach could be adapted to adjust the reactivity distribution of DOC as it transitions from soil to stream conditions, enabling the tracking of further DOC degradation once it enters the streamflow.

The relatively small size of the OSB catchment (25 km^2) enabled certain model simplifications. First, we assumed that the transit time of water at the catchment outlet is equivalent to the time water spends within the soil, thus allowing us to disregard the short transit time within the stream itself. Consequently, the model focuses on degradation processes occurring within the soil, neglecting those within the stream. Second, we assumed that the DOC collected in the streamflow is primarily of terrestrial origin, allowing us to exclude instream sources. This enabled modeling DOC quantity and quality with a focus on soil sources, simulating degradation along the hydrological pathway from the superficial soil layer to the catchment outlet. This second assumption is supported by the PARAFAC analysis results, which show that instream sources (component C_5) account on average for only 7.4% of sampled DOC, and confirmed by the previous analysis conducted on the same dataset in the OSB basin by

Fasching et al. (2016). Additionally, this component acts as a nearly constant baseline concentration and does not significantly contribute to DOC concentration fluctuations. While these assumptions are considered suitable for this case study, they should be carefully evaluated before applying the model to other catchments. In particular, larger catchments may require explicit consideration of terrestrial DOC degradation within the stream network. A possible model development to address this could involve using the current model to produce the DOC concentration and reactivity from lateral discharge along the stream network. The further time evolution of this DOC reactivity spectrum, suitably transformed to account for different environmental conditions (as discussed above), could then be tracked using the transit time within the streamflow as the driving variable. This framework could also incorporate instream sources if the PARAFAC analysis reveals their substantial contribution, a scenario that may be more likely in larger catchments. Expanding the model to include instream sources would involve mapping a proxy for these sources along the network, such as one proportional to gross primary production, and defining an initial reactivity distribution for this DOC input.

5. Conclusions

Our study investigates the quantity and characteristics of terrestrial DOC delivered to streams via lateral fluxes, aiming to clarify DOC dynamics within a second-order alpine stream catchment. The key findings can be summarized as follows:

- Our framework successfully models temporal fluctuations in riverine DOC by linking water transit time with the degradation time of DOC exported from the soil. Additionally, the model's predictions for the average reactivity of exported DOC show a significant relationship with fluorescence and absorbance quality indices independently derived from observed data.
- The predicted reactivity effectively captures the overall variation in the terrestrial DOC quality signature across different discharge regimes, including sequences of low- and high-flow conditions and snowmelt events, although certain aspects of DOC quality dynamics remain unrepresented.
- We compared the changes in DOC reactivity distribution throughout the degradation process with the abundance of terrestrial PARAFAC components, suggesting that our implementation of the reactivity continuum may serve as an initial step in characterizing soil DOC properties. However, we underscore the need for caution in these interpretations, as understanding DOC quality and degradation history remains incomplete.
- The results suggest that water age can serve as a useful proxy for predicting riverine DOC behavior under diverse hydrologic conditions.
- Although our study has focused on small headwater catchments, where in-stream contributions to DOC dynamics can reasonably be neglected, we believe that the framework introduced by Grandi and Bertuzzo (2022) and further developed here represents a significant step forward in quantifying terrestrial DOC export and degradation. This framework provides a foundation for assessing the impact of terrestrial DOC inputs on riverine ecosystems and the potential CO_2 outgassing resulting from in-stream respiration.

Data Availability Statement

Data used in this work and collected by Fasching et al. (2016) in the Oberer Seebach thalweg (Austria) are publicly available at the Zenodo repository "Oberer Seebach dissolved organic carbon dataset" Version v2, at https://doi.org/10.5281/zenodo.10000105 under Creative Commons Attribution 4.0 International license. The repository contains concentrations of riverine and hyporeic DOC at 6-hr time step, measured river gauges at short-time intervals (minutes) and the corresponding discharge and absorbance spectra for each riverine DOC sample. The subfolder "EEMs" gathers together all the Excitation Emission Matrices for riverine DOC samples corrected for Milli-Q water blanks and the inner-filter effects but not for scatters. Finally, a summary of the validated PARAFAC model fitted on the DOC samples is included in the repository and published in OpenFluor with ID number 15640 (pending publication).

Rainfall and air temperature records at the Lunz am See meteorological station are available under Creative Commons Attribution 4.0 International license thanks to the Zentralanstalt für Meteorologie und Geodynamik (ZAMG) at https://data.hub.geosphere.at/dataset/klima-v1-10min.

Acknowledgments
GG and EB carried out this study within the PNRR research activities of the consortium iNEST (Interconnected North-East Innovation Ecosystem) funded by the European Union Next-GenerationEU (Piano Nazionale di Ripresa e Resilienza (PNRR) Missione 4 Componente 2, Investimento 1.5 D.D. 058 23/06/2022, ECS_00000043). This manuscript reflects only the Authors views and opinions, neither the European Union nor the European Commission can be considered responsible for them. SB work was supported by the Spanish Government and the EU Next Generation funding through the EVASIONA and RIPAMED projects (PID-2021-122817NB-100, CNS2023-144737). Open access publishing facilitated by Universita Ca' Foscari, as part of the Wiley - CRUI-CARE agreement.

References

Baker, A., & Spencer, R. G. (2004). Characterization of dissolved organic matter from source to sea using fluorescence and absorbance spectroscopy. *Science of the Total Environment*, *333*(1), 217–232. https://doi.org/10.1016/j.scitotenv.2004.04.013

Barnett, T. P., Adam, J. C., & Lettenmaier, D. P. (2005). Potential impacts of a warming climate on water availability in snow-dominated regions. *Nature*, *438*(7066), 303–309. https://doi.org/10.1038/nature04141

Battin, T. J. (1999). Hydrologic flow paths control dissolved organic carbon fluxes and metabolism in an alpine stream hyporheic zone. *Water Resources Research*, *35*(10), 3159–3169. https://doi.org/10.1029/1999WR900144

Battin, T. J., Lauerwald, R., Bernhardt, E. S., Bertuzzo, E., Gener, L. G., Hall Jr, R. O., et al. (2023). River ecosystem metabolism and carbon biogeochemistry in a changing world. *Nature*, *613*(7944), 449–459. https://doi.org/10.1038/s41586-022-05500-8

Battin, T. J., Luyssaert, S., Kaplan, L., Audfenkampe, A., Richter, A., & Tranvik, L. (2009). The boundless carbon cycle. *Nature Geoscience*, *2*(9), 598–600. https://doi.org/10.1038/ngeo618

Benettin, P., & Bertuzzo, E. (2018). *tran*-SAS v1.0: A numerical model to compute catchment-scale hydrologic transport using StorAge Selection functions. *Geoscientific Model Development*, *11*(4), 1627–1639. https://doi.org/10.5194/gmd-11-1627-2018

Benettin, P., Rodriguez, N. B., Sprenger, M., Kim, M., Klaus, J., Harman, C. J., et al. (2022). Transit time estimation in catchments: Recent developments and future directions. *Water Resources Research*, *58*(11), e2022WR033096. https://doi.org/10.1029/2022WR033096

Benettin, P., Soulsby, C., Birkel, C., Tetzlaff, D., Botter, G., & Rinaldo, A. (2017). Using SAS functions and high-resolution isotope data to unravel travel time distributions in headwater catchments. *Water Resources Research*, *53*(3), 1864–1878. https://doi.org/10.1002/2016WR020117

Berggren, M., Guillemette, F., Bieroza, M., Buffam, I., Deininger, A., Hawkes, J. A., et al. (2022). Unified understanding of intrinsic and extrinsic controls of dissolved organic carbon reactivity in aquatic ecosystems. *Ecology*, *103*(9), e3763. https://doi.org/10.1002/ecy.3763

Bolan, N. S., Adriano, D. C., Kunhikrishnan, A., James, T., McDowell, R., & Senesi, N. (2011). Dissolved organic matter: Biogeochemistry, dynamics, and environmental significance in soils. *Advances in Agronomy*, *110*, 1–75.

Botter, G., Porporato, A., Rodriguez-Iturbe, I., & Rinaldo, A. (2009). Nonlinear storage-discharge relations and catchment streamflow regimes. *Water Resources Research*, *45*(10). https://doi.org/10.1029/2008WR007658

Boyer, E. W., Hornberger, G. M., Bencala, K. E., & McKnight, D. M. (1997). Response characteristics of DOC flushing in an alpine catchment. *Hydrological Processes*, *11*(12), 1635–1647. https://doi.org/10.1002/(SICI)1099-1085(19971015)11:12⟨1635::AID-HYP494⟩3.0.CO;2-H

Boyer, E. W., Hornberger, G. M., Bencala, K. E., & McKnight, D. M. (2000). Effects of asynchronous snowmelt on flushing of dissolved organic carbon: A mixing model approach. *Hydrological Processes*, *14*(18), 3291–3308. https://doi.org/10.1002/1099-1085(20001230)14:18⟨3291::AID-HYP202⟩3.0.CO;2-2

Bretschko, G. (1991). The limnology of a low order alpine gravel stream (ritrodat-lunz study area, Austria). *SIL Proceedings, 1922-2010*, *24*(3), 1908–1912. https://doi.org/10.1080/03680770.1989.11899095

Bro, R. (1997). PARAFAC. tutorial and applications. *Chemometrics and Intelligent Laboratory Systems*, *38*(2), 149–171. https://doi.org/10.1016/S0169-7439(97)00032-4

Brutsaert, W., & Nieber, J. L. (1977). Regionalized drought flow hydrographs from a mature glaciated plateau. *Water Resources Research*, *13*(3), 637–644. https://doi.org/10.1029/WR013i003p00637

Butturini, A., Gallart, F., Latron, J., Vazquez, E., & Sabater, F. (2006). Cross-site comparison of variability of DOC and nitrate c-q hysteresis during the autumn–winter period in three mediterranean headwater streams: A synthetic approach. *Biogeochemistry*, *77*(3), 327–349. https://doi.org/10.1007/s10533-005-0711-7

Campbell, J. L., Reinmann, A. B., & Templer, P. H. (2014). Soil freezing effects on sources of nitrogen and carbon leached during snowmelt. *Soil Science Society of America Journal*, *78*(1), 297–308. https://doi.org/10.2136/sssaj2013.06.0218

Carey, S. K. (2003). Dissolved organic carbon fluxes in a discontinuous permafrost subarctic alpine catchment. *Permafrost and Periglacial Processes*, *14*(2), 161–171. https://doi.org/10.1002/ppp.444

Catalán, N., Obrador, B., Felip, M., & Pretus, J. L. (2013). Higher reactivity of allochthonous vs. autochthonous DOC sources in a shallow lake. *Aquatic Sciences*, *75*(4), 581–593. https://doi.org/10.1007/s00027-013-0302-y

Catalán, N., Pastor, A., Borrego, C. M., Casas-Ruiz, J. P., Hawkes, J. A., Gutiérrez, C., et al. (2021). The relevance of environment vs. composition on dissolved organic matter degradation in freshwaters. *and Oceanography*, *66*(2), 306–320. https://doi.org/10.1002/lno.11606

Cawley, K. M., Ding, Y., Fourqurean, J., & Jaffé, R. (2012). Characterising the sources and fate of dissolved organic matter in Shark Bay, Australia: A preliminary study using optical properties and stable carbon isotopes. *Marine and Freshwater Research*, *63*(11), 1098–1107. https://doi.org/10.1071/mf12028

Chen, M., & Jaffé, R. (2014). Photo- and bio-reactivity patterns of dissolved organic matter from biomass and soil leachates and surface waters in a subtropical wetland. *Water Research*, *61*, 181–190. https://doi.org/10.1016/j.watres.2014.03.075

Coble, P. G. (1996). Characterization of marine and terrestrial DOM in seawater using excitation-emission matrix spectroscopy. *Marine Chemistry*, *51*(4), 325–346. https://doi.org/10.1016/0304-4203(95)00062-3

Cole, J., Prairie, Y., Caraco, N., McDowell, W., Tranvik, L., Striegl, R., et al. (2007). 05). Plumbing the global carbon cycle: Integrating inland waters into the terrestrial carbon budget. *Ecosystems*, *10*(1), 172–185. https://doi.org/10.1007/s10021-006-9013-8

Dawson, J., Soulsby, C., Tetzlaff, D., Hrachowitz, M., Dunn, S., & Malcolm, I. (2008). Influence of hydrology and seasonality on DOC exports from three contrasting upland catchments. *Biogeochemistry*, *90*(1), 93–113. https://doi.org/10.1007/s10533-008-9234-3

Fasching, C., Behounek, B., Singer, G. A., & Battin, T. J. (2014). Microbial degradation of terrigenous dissolved organic matter and potential consequences for carbon cycling in brown-water streams. *Scientific Reports*, *4*(1), 4981. https://doi.org/10.1038/srep04981

Fasching, C., Ulseth, A. J., Schelker, J., Steniczka, G., & Battin, T. J. (2016). Hydrology controls dissolved organic matter export and composition in an Alpine stream and its hyporheic zone. *and Oceanography*, *61*(2), 558–571. https://doi.org/10.1002/lno.10232

Finlay, J., Neff, J., Zimov, S., Davydova, A., & Davydov, S. (2006). Snowmelt dominance of dissolved organic carbon in high-latitude watersheds: Implications for characterization and flux of river doc. *Geophysical Research Letters*, *33*(10). https://doi.org/10.1029/2006GL025754

Galletti, Y., Gonnelli, M., Retelletti Brogi, S., Vestri, S., & Santinelli, C. (2019). DOM dynamics in open waters of the mediterranean sea: New insights from optical properties. *Deep Sea Research Part I: Oceanographic Research Papers*, *144*, 95–114. https://doi.org/10.1016/j.dsr.2019.01.007

Gao, Z., & Guéguen, C. (2017). Size distribution of absorbing and fluorescing DOM in Beaufort sea, Canada basin. *Deep Sea Research Part I: Oceanographic Research Papers*, *121*, 30–37. https://doi.org/10.1016/j.dsr.2016.12.014

Gentine, P., Green, J. K., Guérin, M., Humphrey, V., Seneviratne, S. I., Zhang, Y., & Zhou, S. (2019). Coupling between the terrestrial carbon and water cycles—A review. *Environmental Research Letters*, *14*(8), 083003. https://doi.org/10.1088/1748-9326/ab22d6

Grandi, G., & Bertuzzo, E. (2022). Catchment dissolved organic carbon transport: A modeling approach combining water travel times and reactivity continuum. *Water Resources Research*, *58*(7), e2021WR031275. https://doi.org/10.1029/2021wr031275

Gros, M., Catalán, N., Mas-Pla, J., Čelić, M., Petrović, M., & Farré, M. J. (2021). Groundwater antibiotic pollution and its relationship with dissolved organic matter: Identification and environmental implications. *Environmental Pollution*, *289*, 117927. https://doi.org/10.1016/j.envpol.2021.117927

Hanus, S., Hrachowitz, M., Zekollari, H., Schoups, G., Vizcaino, M., & Kaitna, R. (2021). Future changes in annual, seasonal and monthly runoff signatures in contrasting alpine catchments in Austria. *Hydrology and Earth System Sciences*, *25*(6), 3429–3453. https://doi.org/10.5194/hess-25-3429-2021

Harman, C. J. (2015). Time-variable transit time distributions and transport: Theory and application to storage-dependent transport of chloride in a watershed. *Water Resources Research*, *51*(1), 1–30. https://doi.org/10.1002/2014WR015707

Hemingway, J. D., Spencer, R. G., Podgorski, D. C., Zito, P., Sen, I. S., & Galy, V. V. (2019). Glacier meltwater and monsoon precipitation drive upper ganges basin dissolved organic matter composition. *Geochimica et Cosmochimica Acta*, *244*, 216–228. https://doi.org/10.1016/j.gca.2018.10.012

Hood, E., Battin, T. J., Fellman, J., O'neel, S., & Spencer, R. G. (2015). Storage and release of organic carbon from glaciers and ice sheets. *Nature Geoscience*, *8*(2), 91–96. https://doi.org/10.1038/ngeo2331

Horgby, Å., Segatto, P. L., Bertuzzo, E., Lauerwald, R., Lehner, B., Ulseth, A. J., et al. (2019). Unexpected large evasion fluxes of carbon dioxide from turbulent streams draining the world's mountains. *Nature Communications*, *10*(1), 4888. https://doi.org/10.1038/s41467-019-12905-z

Houser, J. N., Bade, D. L., Cole, J. J., & Pace, M. L. (2003). The dual influences of dissolved organic carbon on hypolimnetic metabolism: Organic substrate and photosynthetic reduction. *Biogeochemistry*, *64*(2), 247–269.

Hrachowitz, M., Fovet, O., Ruiz, L., & Savenije, H. H. (2015). Transit time distributions, legacy contamination and variability in biogeochemical 1/fα scaling: How are hydrological response dynamics linked to water quality at the catchment scale? *Hydrological Processes*, *29*(25), 5241–5256. https://doi.org/10.1002/hyp.10546

Hrachowitz, M., Stockinger, M., Coenders-Gerrits, M., van der Ent, R., Bogena, H., Lücke, A., & Stumpp, C. (2021). Reduction of vegetation-accessible water storage capacity after deforestation affects catchment travel time distributions and increases young water fractions in a headwater catchment. *Hydrology and Earth System Sciences*, *25*(9), 4887–4915. https://doi.org/10.5194/hess-25-4887-2021

Kalbitz, K., Solinger, S., Park, J.-H., Michalzik, B., & Matzner, E. (2000). Controls on the dynamics of dissolved organic matter in soils: A review. *Soil Science*, *165*(4), 277–304. https://doi.org/10.1097/00010694-200004000-00001

Kaplan, L. A., Newbold, J. D., Horn, D. J. V., Dow, C. L., Aufdenkampe, A. K., & Jackson, J. K. (2006). Organic matter transport in New York City drinking-water-supply watersheds. *Journal of the North American Benthological Society*, *25*(4), 912–927. https://doi.org/10.1899/0887-3593(2006)025[0912:OMTINY]2.0.CO;2

Kirchner, J. W. (2009). Catchments as simple dynamical systems: Catchment characterization, rainfall-runoff modeling, and doing hydrology backward. *Water Resources Research*, *45*(2). https://doi.org/10.1029/2008wr006912

Kirchner, J. W. (2016). Aggregation in environmental systems–part 1: Seasonal tracer cycles quantify young water fractions, but not mean transit times, in spatially heterogeneous catchments. *Hydrology and Earth System Sciences*, *20*(1), 279–297. https://doi.org/10.5194/hess-20-279-2016

Korak, J. A., & McKay, G. (2024). Critical review of fluorescence and absorbance measurements as surrogates for the molecular weight and aromaticity of dissolved organic matter. *Environmental Sciences: Processes and Impacts*, *26*(10), 1663–1702. https://doi.org/10.1039/D4EM00183D

Kothawala, D. N., Stedmon, C. A., Müller, R. A., Weyhenmeyer, G. A., Köhler, S. J., & Tranvik, L. J. (2014). Controls of dissolved organic matter quality: Evidence from a large-scale boreal lake survey. *Global Change Biology*, *20*(4), 1101–1114. https://doi.org/10.1111/gcb.12488

Kowalczuk, P., Stedmon, C. A., & Markager, S. (2006). Modeling absorption by CDOM in the Baltic Sea from season, salinity and chlorophyll. *Marine Chemistry*, *101*(1), 1–11. https://doi.org/10.1016/j.marchem.2005.12.005

Leichtfried, M. (1996). 09). Organic matter in bed-sediments of the river danube and a small unpolluted stream, the obeyer seebach. *Large Rivers*, *10*(1–4), 87–98. https://doi.org/10.1127/lr/10/1996/87

Lupon, A., Denfeld, B. A., Laudon, H., Leach, J., Karlsson, J., & Sponseller, R. A. (2019). Groundwater inflows control patterns and sources of greenhouse gas emissions from streams. *and Oceanography*, *64*(4), 1545–1557. https://doi.org/10.1002/lno.11134

Marín-Spiotta, E., Gruley, K., Crawford, J., Atkinson, E., Miesel, J., Greene, S., et al. (2014). Paradigm shifts in soil organic matter research affect interpretations of aquatic carbon cycling: Transcending disciplinary and ecosystem boundaries. *Biogeochemistry*, *117*(2–3), 279–297. https://doi.org/10.1007/s10533-013-9949-7

Maritorena, S., Siegel, D. A., & Peterson, A. R. (2002). Optimization of a semianalytical ocean color model for global-scale applications. *Applied Optics*, *41*(15), 2705–2714. https://doi.org/10.1364/AO.41.002705

Murphy, K. R., Bro, R., & Stedmon, C. A. (2014). Chemometric analysis of organic matter fluorescence. *Aquatic Organic Matter Fluorescence*, *261*(1), 339–375. https://doi.org/10.1017/cbo9781139045452.016

Murphy, K. R., Stedmon, C. A., Graeber, D., & Bro, R. (2013). Fluorescence spectroscopy and multi-way techniques. *PARAFAC. Analytical Methods*, *5*(23), 6557–6566. https://doi.org/10.1039/C3AY41160E

Rango, A., & Martinec, J. (1995). Revisiting the degree-day method for snowmelt computations 1. *JAWRA Journal of the American Water Resources Association*, *31*(4), 657–669. https://doi.org/10.1111/j.1752-1688.1995.tb03392.x

Raymond, P., & Saiers, J. (2010). Event controlled DOC export from forested watersheds. *Biogeochemistry*, *100*(1–3), 197–209. https://doi.org/10.1007/s10533-010-9416-7

Rinaldo, A., Benettin, P., Harman, C. J., Hrachowitz, M., McGuire, K. J., Van Der Velde, Y., et al. (2015). StorAge selection functions: A coherent framework for quantifying how catchments store and release water and solutes. *Water Resources Research*, *51*(6), 4840–4847. https://doi.org/10.1002/2015WR017273

Robison, A. L., Deluigi, N., Rolland, C., Manetti, N., & Battin, T. (2023). Glacier loss and vegetation expansion alter organic and inorganic carbon dynamics in high-mountain streams. *Biogeosciences*, *20*(12), 2301–2316. https://doi.org/10.5194/bg-20-2301-2023

Segatto, P. L., Battin, T. J., & Bertuzzo, E. (2023). A network-scale modeling framework for stream metabolism, ecosystem efficiency, and their response to climate change. *Water Resources Research*, *59*(3), e2022WR034062. https://doi.org/10.1029/2022WR034062

Shanley, J. B., Alisa Mast, M., Campbell, D. H., Aiken, G. R., Krabbenhoft, D. P., Hunt, R. J., et al. (2008). Comparison of total mercury and methylmercury cycling at five sites using the small watershed approach. *Environmental Pollution*, *154*(1), 143–154. (Mercury Cycling and Bioaccumulation in the Environment). https://doi.org/10.1016/j.envpol.2007.12.031

Shatilla, N. J., & Carey, S. K. (2019). Assessing inter-annual and seasonal patterns of DOC and DOM quality across a complex alpine watershed underlain by discontinuous permafrost in yukon, Canada. *Hydrology and Earth System Sciences*, *23*(9), 3571–3591. https://doi.org/10.5194/hess-23-3571-2019

Snucins, E., & Gunn, J. (2000). Interannual variation in the thermal structure of clear and colored lakes. *and Oceanography*, *45*(7), 1639–1646. https://doi.org/10.4319/lo.2000.45.7.1639

Stewart, B., Shanley, J. B., Kirchner, J. W., Norris, D., Adler, T., Bristol, C., et al. (2022). Streams as mirrors: Reading subsurface water chemistry from stream chemistry. *Water Resources Research*, *58*(1), e2021WR029931. https://doi.org/10.1029/2021WR029931

ter Braak, C. J., & Vrugt, J. A. (2008). Differential evolution Markov chain with snooker updater and fewer chains. *Statistics and Computing*, *18*(4), 435–446. https://doi.org/10.1007/s11222-008-9104-9

Ulseth, A. J., Bertuzzo, E., Singer, G. A., Schelker, J., & Battin, T. J. (2018). Climate-induced changes in spring snowmelt impact ecosystem metabolism and carbon fluxes in an alpine stream network. *Ecosystems*, *21*(2), 373–390. https://doi.org/10.1007/s10021-017-0155-7

van der Velde, Y., Heidbuchel, I., Lyon, S. W., Nyberg, L., Rodhe, A., Bishop, K., & Troch, P. A. (2014). Consequences of mixing assumptions for time-variable travel time distributions. *Hydrological Processes*, *29*(16), 3460–3474. https://doi.org/10.1002/hyp.10372

Vrugt, J. A., Ter Braak, C., Diks, C., Robinson, B. A., Hyman, J. M., & Higdon, D. (2009). Accelerating Markov chain Monte Carlo simulation by differential evolution with self-adaptive randomized subspace sampling. *International Journal of Nonlinear Sciences and Numerical Stimulation*, *10*(3), 273–290. https://doi.org/10.1515/IJNSNS.2009.10.3.273

Ward, N. D., Keil, R. G., Medeiros, P. M., Brito, D. C., Cunha, A. C., Dittmar, T., et al. (2013). Degradation of terrestrially derived macromolecules in the amazon river. *Nature Geoscience*, *6*(7), 530–533. https://doi.org/10.1038/ngeo1817

Wei, X., Hayes, D. J., Butman, D. E., Qi, J., Ricciuto, D. M., & Yang, X. (2024). Modeling exports of dissolved organic carbon from landscapes: A review of challenges and opportunities. *Environmental Research Letters*, *19*(5), 053001. https://doi.org/10.1088/1748-9326/ad3cf8

Weishaar, J. L., Aiken, G. R., Bergamaschi, B. A., Fram, M. S., Fujii, R., & Mopper, K. (2003). Evaluation of specific ultraviolet absorbance as an indicator of the chemical composition and reactivity of dissolved organic carbon. *Environmental Science and Technology*, *37*(20), 4702–4708. https://doi.org/10.1021/es030360x

Wen, H., Perdrial, J., Abbott, B. W., Bernal, S., Dupas, R., Godsey, S. E., et al. (2020). Temperature controls production but hydrology regulates export of dissolved organic carbon at the catchment scale. *Hydrology and Earth System Sciences*, *24*(2), 945–966. https://doi.org/10.5194/hess-24-945-2020

Wrona, F. J., Johansson, M., Culp, J. M., Jenkins, A., Mård, J., Myers-Smith, I. H., et al. (2016). Transitions in arctic ecosystems: Ecological implications of a changing hydrological regime. *Journal of Geophysical Research: Biogeosciences*, *121*(3), 650–674. https://doi.org/10.1002/2015JG003133

Wünsch, U. J., & Murphy, K. (2021). A simple method to isolate fluorescence spectra from small dissolved organic matter datasets. *Water Research*, *190*, 116730. https://doi.org/10.1016/j.watres.2020.116730

Yamashita, Y., Kloeppel, B. D., Knoepp, J., Zausen, G. L., & Jaffé, R. (2011). Effects of watershed history on dissolved organic matter characteristics in headwater streams. *Ecosystems*, *14*(7), 1110–1122. https://doi.org/10.1007/s10021-011-9469-z

Yamashita, Y., Kojima, D., Yoshida, N., & Shibata, H. (2021). Relationships between dissolved black carbon and dissolved organic matter in streams. *Chemosphere*, *271*, 129824. https://doi.org/10.1016/j.chemosphere.2021.129824

Zsolnay, A., Baigar, E., Jimenez, M., Steinweg, B., & Saccomandi, F. (1999). Differentiating with fluorescence spectroscopy the sources of dissolved organic matter in soils subjected to drying. *Chemosphere*, *38*(1), 45–50. https://doi.org/10.1016/s0045-6535(98)00166-0